Available online at www.sciencedirect.com
SCIENCE DIRECT®
Fluid Phase Equilibria 222–223 (2004) 107–118
FLUID PHASE EQUILIBRIA
www.elsevier.com/locate/fluid

Universal equation of state for engineering application: algorithm and application to non-polar and polar fluids

Lixin Sun, James F. Ely*

Department of Chemical Engineering, Colorado School of Mines, Golden, CO 80401, USA

Abstract

Engineering equations of state (EOS) deal with the majority of fluids of interest in process and equipment design in the chemical industries. Accuracy and universality are two desirable features the engineering EOS require, however, both of them cannot be simultaneously obtained without some degree of compromise. Therefore a simultaneous optimization algorithm is proposed to develop an accurate but compact engineering EOS for wide range of fluids with one single functional form. The algorithm is based on a simulated annealing method, and operates on different fluids at the same time to achieve the best average results. A 14-term EOS is developed based on this algorithm that has good accuracy for selected non-polar and polar fluids. The resulting equation is compared with two different 12-term EOS developed by Span and Wagner, one for polar fluids, the other for non-polar fluids. The new 14-term EOS also gives good predictions for some associating fluids such as alcohols and water.
© 2004 Elsevier B.V. All rights reserved.

Keywords: Equation of state; Optimization algorithm; Non-polar and polar fluids; Associating fluids; Thermodynamic properties

1. Introduction

Engineering equations of state (EOS) generally refer to those equations used for equipment and process design. Their accuracy is lower than that achieved with state-of-the-art reference EOS, which predict thermodynamic properties to within experimental uncertainty. An advantage of the engineering EOS is that they typically have a simpler mathematical structure than found in a reference quality equation. As pointed out by other researchers [1,2], highly accurate reference EOS have only been developed for a few fluids for which extensive and accurate experimental measurements are available. For the majority of industrially interesting fluids, these reference EOS will not be developed in the foreseeable future, and in some cases it is even difficult to develop an engineering quality EOS for many of these fluids due to the paucity of experimental data. Even though accuracy is an important requirement for an EOS, universality, i.e., fixed functional form, is another desired feature. A universal engineering EOS which is applicable to a wide range of fluid systems can easily fit into current process design and control packages, and can be easily applied when new fluid data become available.

Cubic EOS like the Redlich–Kwong [3], Soave–Redlich-Kwong [4], and Peng–Robinson [5], etc., are types of engineering EOS that are used widely in industry, primarily due to their simple structure. With three substance-specific parameters, these equations give qualitatively correct results. The Benedict–Webb–Rubbin (BWR)- [6], Starling- [7] or Bender-type [8] EOS have relatively higher accuracy and are also popular in industry. Polt [9] and Plater [10] report sets of coefficients for 51 non-polar and polar fluids for the Bender equation of state. Although these generalized Bender-type equations give reasonably accurate predictions for thermodynamic properties, they cannot be extrapolated to regions where experimental data have not been used in the development of the parameters. Even within the range where reliable $P\rho T$ data are available, the Bender-type equations can give unreasonable predictions of the isobaric heat capacity in the high temperature region [11]. The main reason for this behavior is that neither the Bender nor other BWR-type equations are structure optimized and there are severe correlations among the coefficients.

* Corresponding author. Tel.: +1 303 273 3720; fax: +1 303 273 3730.
E-mail address: jely@mines.edu (J.F. Ely).

0378-3812/$ – see front matter © 2004 Elsevier B.V. All rights reserved.
doi:10.1016/j.fluid.2004.06.028

Modern algorithms for the development of reference EOS enable the reduction of intercorrelations in an EOS giving superior accuracy and numerical stability. However the success of these algorithms, like the OPTIM proposed by Setzmann and Wagner [12], heavily depends on the availability of data for the fluids of interest. More importantly, these algorithms can only develop one reference EOS for one specified fluid at a time. In order to cover a broader range of fluids, the EOS has to be transformed to be applied to other fluids. Usually when an EOS for substance A is applied to substance B, it loses its accuracy and numerical stability.

Span and Wagner [11,13] proposed a simultaneous optimization algorithm, the SIMOPT, to develop accurate and numerically stable engineering equations for multiple fluids at the same time. The SIMOPT algorithm is based on the OPTIM algorithm and completely identical to the OPTIM algorithm with respect to data and constraints. Regression matrices are setup for each individual fluid with the same bank of terms. Since the optimization algorithm manipulates the terms only by their positions in the bank of terms, the regression matrices are transformed in exactly the same way for each fluid during regression. The difference between the SIMOPT and the OPTIM lies in the way the algorithm handles the merit function or the quality criteria [11,13] and the statistical tests.

Span and Wagner applied the SIMOPT algorithm to a group of 15 non- and weakly polar fluids and a group of 13 polar fluids, and generated two engineering EOS, one for each group of fluids [11,14,15]. These two engineering EOS give surprisingly good accuracy and good numerical stability with merely 12 functional terms in each of them.

Despite the success of Span and Wagner's approach, there are still drawbacks regarding the algorithm and resulting engineering EOS. As mentioned by Span and Wagner [11,13], reference sums of squares are needed to create the quality criteria in the SIMOPT algorithm, which are not readily available and require EOS fitting for individual fluids. The heart of the SIMOPT is based on a combination of stepwise regression and the evolutionary optimization method, which makes the algorithm as complex as the OPTIM algorithm. In addition, the scope of the fluids studied is still limited to alkanes, light inorganics and refrigerants; aromatic hydrocarbons and associating fluids were not included.

As mentioned earlier, universality is another important feature for an engineering EOS. The two 12-term engineering EOS obtained by Span and Wagner [11,14,15] are totally different EOS and cannot be used across groups. Also Bonsen et al. [16] report that associating fluids such as alcohols and water cannot be modeled with these two EOS.

The objective of this work is to use the simulated annealing to develop a single engineering EOS that yields the same accuracy as that obtained by Span and Wagner, but covers a broader range of fluids. We proceed as follows. In Section 2 we describe the simulated annealing technique and its application in the development of equations of state. The proposed simultaneous optimization algorithm is given in Section 3. We then present the resulting engineering EOS together with comparisons to experimental data and Span and Wanger's results in Section 4. Conclusions are summarized in Section 5.

2. Development of equation of state by simulated annealing

Deterministic algorithms like stepwise regression frequently end up with a local rather than global minimum, especially when the functional form of an EOS can have many independent variables. Compared to stepwise regression, simulated annealing (SA) is quite simple and has been used in a variety of applications in combinatorial optimization. Its potential advantage is that it can find global minima and it can be easily combined with parallel regressions to develop a universal EOS.

Simulated annealing was first developed to optimize circuit design by Kirkpatrick et al. [17], and independently by Cerny [18]. In their work, Kirkpatrick et al. used the principles of statistical mechanics to solve combinatorial optimization problems. The method is implemented using the Metropolis algorithm [19], which is widely used in atomic scale Monte Carlo simulation. In its application a change of state (configuration at the atomistic level) is accepted according to the following rule:

$$p = 1, \quad \Delta C \leq 0, \qquad p = \mathrm{e}^{-\Delta C/T}, \quad \Delta C > 0 \tag{1}$$

where p is the probability that a configuration is accepted, ΔC the change of the function to be minimized (cost function—originally ΔU at the atomistic level) and T the temperature. If p is less than one but greater than R, a randomly generated number between 0 and 1, the move is also accepted. If p is less than the random number R, the move is rejected. Such a probabilistic rule allows uphill steps to be accepted if the probability is larger than a random number between (0, 1). Thus the method is able to move out of a local minimum at nonzero temperatures. Shubert and Ely [20] applied the simulated annealing method to develop reference equations of state for refrigerants R134a and R123.

The equation of state developed in this work is expressed as a Helmholtz free energy function of density and temperature. The Helmholtz free energy can be described as a linear combination of the ideal gas (id) and residual or real fluid (r) contributions where the latter arise due to intermolecular interactions. Mathematically,

$$A(\rho, T) = A^{\mathrm{id}}(\rho, T) + A^{\mathrm{r}}(\rho, T) \tag{2}$$

where A is the Helmholtz free energy, and ρ and T are the density and temperature, respectively. Generally the Helmholtz function is formulated in dimensionless form as

$$\Phi \equiv \frac{A(\rho, T)}{RT} = \Phi^{\mathrm{id}}(\delta, t) + \Phi^{\mathrm{r}}(\delta, t) \tag{3}$$

where $\delta = \rho/\rho_r$ and $t = T_r/T$. The reference density ρ_r and temperature T_r are usually chosen to be the critical parameters ρ_c and T_c.

The ideal part of Helmholtz energy is determined from experimental or theoretical knowledge of the ideal gas heat capacity as follows:

$$\Phi^{id} = \frac{A^{id}(\rho, T)}{RT} = \ln\left(\frac{\rho}{\rho_0}\right) + \int \frac{C_p^0}{T} dT \quad (4)$$

The residual part of the Helmholtz equation is assumed to be a linear combination of dimensionless density and temperature terms (so-called "functional terms") as shown in Eq. (5),

$$\Phi^r(\delta, t) = \sum_{m=1}^{M_1} a_m \delta^{i_m} t^{j_m} + \sum_{m=M_1+1}^{M_2} a_m \delta^{i_m} t^{j_m} \exp(-\delta^{k_m}) \quad (5)$$

where a_m is the coefficient for each term, i_m, j_m and k_m are exponents on t, δ and exponential δ terms, respectively, and M_1 and M_2 are the numbers of different type of terms. As can be seen from this equation, the two types of terms are polynomial and exponential. A decision algorithm like simulated annealing in conjunction with a regression algorithm is used to determine the number of parameters and their values.

When dealing with the development of an EOS, the change of cost function ΔC in simulated annealing is defined as the variance of the equation of state at each regression step k,

$$C = \frac{S^2}{N_f} \quad (6)$$

where N_f refers to the degrees of freedom, and can be calculated as

$$N_f = N_{data} - N_{constr} - N_{term} \quad (7)$$

where N_{data} is the total number of data points used in the regression, N_{constr} the number of constraints and N_{term} the number of function terms in the formulation at regression step k. The weighted sum of squared residual from the linear regression, S^2, is given as

$$S^2 = \sum_{n=1}^{N_{data}} W_n (Y_n - y_n)^2 \quad (8)$$

where W_n is the total weight of data point n, Y_n the experimental value at that point, and y_n is the value calculated from the regressed equation of state.

The EOS simulated annealing algorithm has four main operations. The first step is initialization; i.e., to arbitrarily choose a fixed number of terms as the starting point. The second step is replacement: to randomly select a term from the existing formulation and replace it with a randomly selected term from the collection of possible of terms. The exchange of terms is accepted if the change in the cost function satisfies the acceptance criteria described above. The third step is temperature scheduling: to change temperature according to an annealing schedule which is a sequence of effective temperatures that decrease in slow steps until the objective function reaches a minimum. The annealing schedule has to be carefully chosen to ensure that the system moves to its minimum slowly. The last step in the algorithm is termination. The regression will be terminated if three trials fail to find any improvement in the cost function, or a maximum number of temperature steps is exceeded.

Huber reported the performance of three temperature schedules in conjunction with simulated annealing when developing vapor pressure correlations for R134a in 1994 [21]. The three schedules are an exponential, the Aarts and VanLaarhoven algorithm [22] and the Lundy and Mees algorithm [23]. As pointed out by Huber [21], the simulated annealing with a Lundy and Mees annealing schedule gave the overall best results. Thus, we have chosen to use the Lundy and Mees schedule in this work. The Lundy and Mees algorithm [23] is shown as

$$T_{k+1} = \frac{T_k}{1 + \delta_{LM} T_k} \quad (9)$$

where δ_{LM} is the parameter which controls the annealing speed, T_k and T_{k+1} are the annealing temperature at step k and $k+1$, respectively.

3. Simultaneous optimization algorithm

As mentioned in Section 1, an EOS with optimized structure tends to be more numerically stable and more accurate than the Bender-type equations for a specified fluid. However when the EOS is transferred to other fluids the accuracy and numerical stability can be lost. In order to overcome this problem, we propose an optimization algorithm, MULTIREG, which considers data sets from different fluids simultaneously. The purpose of MULTIREG is to determine an overall best EOS for multiple fluids. The resulting EOS does not favor any specific fluid; instead, it will give on average the best results for all fluids considered (base fluids). Further, the resulting EOS should be able to give good predictions when extended to other fluids in the same groups as the base fluids. For those fluids with limited data sets, the resulting EOS should give at least reasonable predictions in the regions which are not covered by available data, but are covered by the base fluids.

The MULTIREG algorithm is based on linear-least squares regression and simulated annealing. A flow diagram for the development of a technical EOS using MULTIREG algorithm is shown in Fig. 1. The procedures to set up the regression matrices are the same as in the development of multiparameter equation of state described in various references [24–27]. Experimental data sets are processed, and appropriate weights are generated before the data sets are put into separate matrices for each individual substance using the same bank of terms. Critical constraints for each

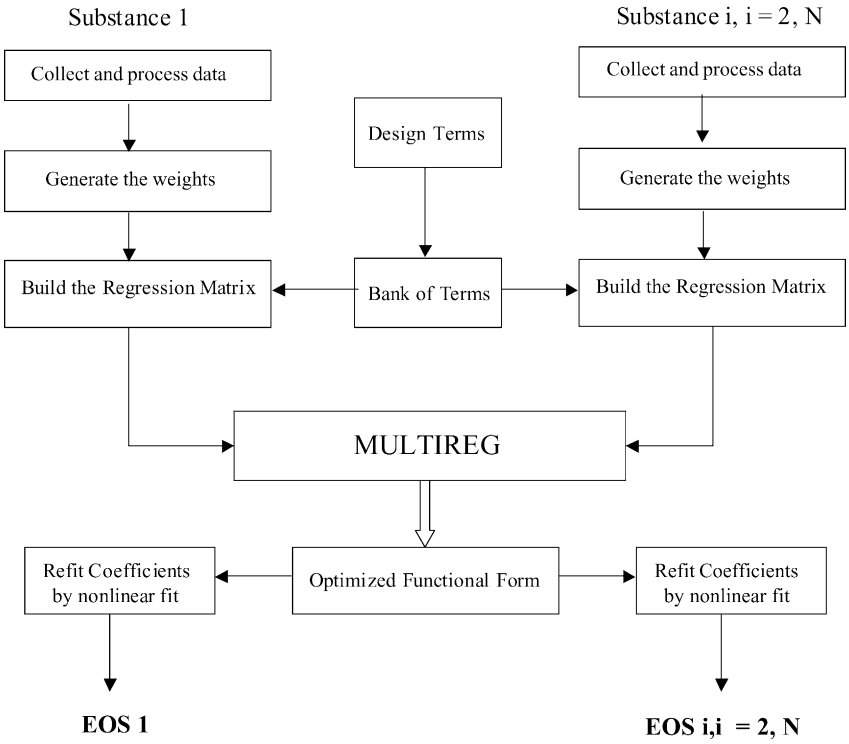

Fig. 1. Flow diagram about the development of engineering equation of state from the MULTIREG algorithm.

fluid are also included in the corresponding normal matrices to ensure the resulting EOS predicts the correct critical points. The critical temperature T_c and density ρ_c are used to reduce the temperature and density of the corresponding fluid.

3.1. Weighting

In the development of reference quality EOS, appropriate weights must be generated to ensure the best linear unbiased (BLUE) results from the linear-least squares regression [26]. In order to develop engineering EOS for multiple fluids, weights should also be generated for data sets of each individual fluid as well. In this work a modified Gaussian error propagation rule was applied, and the total weight for each data point is

$$W_n = \frac{F_T}{\sigma_{r_n}^2} = \frac{F_T}{\sigma_{y_n}^2 + \sum_{k=1}^{K}[(\partial y/\partial x_{nk})\sigma_{x_{nk}}]^2} \tag{10}$$

where $\sigma_{y_n}^2$ is the variance of the dependent variable y_n, ∂x_{nk} the variance of the independent variable x_{nk} and K the number of independent variables. A simplex method [28] is used to find the weighting factors F_T to account for the relative importance of individual data set for each fluid.

As mentioned by Span and Wagner [11,13], the reduced form of the quality criteria S^2 needs to be used to offset any exaggerated influence from the well-measured fluids. To accomplish this extra weighting factors w_i are introduced as follows. After initialization of regression matrix i ($i = 1, I$), the relative percentage $\Delta_i\%$ of each sum of squares S_i^2 is calculated according to

$$\Delta_i\% = \frac{S_i^2}{\sum_{i=1}^{I} S_i^2} \times 100\% \tag{11}$$

Then the extra weighting factor w_i for each substance is obtained from

$$w_i = \frac{\mathrm{MAX}(\Delta_i\%)}{\Delta_i\%} \times 100\% \tag{12}$$

and is used in the calculation of the cost function as described below. In such a way, those fluids with high values of S_i^2 will be assigned a smaller value of w_i so that during optimization they will not receive extra weight in the algorithm and the fluids with smaller values of S_i^2 will be considered equally.

3.2. MULTIREG algorithm

When applying simulated annealing to the development of an EOS for a single fluid i, the cost function C is the variance of the equation of state at each regression step k, as shown in Eqs. (6) and (7). However, when dealing with multiple fluids, the cost function C should have following form:

$$C = \frac{\sum_{i=1}^{I}(S_i^2/N_{fi})w_i}{I} \tag{13}$$

where I is the total number of fluids considered, and w_i the extra weighting factor discussed above.

The change of cost function ΔC from step k to step $(k+1)$ is then calculated from

$$\Delta C = \frac{\sum_{i=1}^{I}((S_{i,k+1}^2 - S_{i,k}^2)/N_{fi})w_i}{I} \quad (14)$$

by using this algorithm the general structure of the MULTIREG algorithm corresponds exactly to the structure of the simulated annealing algorithm for single fluid. As described previously, regression matrices are built using the processed data sets and weights for each fluid with the same bank of terms. At initialization, the pre-selected terms are added to each matrix and the matrices are transformed accordingly. During the initialization, the critical constraints are also added. MULTIREG then randomly chooses a term A from the bank of terms and second random term B in the current formulation, and carries out exchange on each regression matrix. At this stage the exchange is a mock-exchange, which means only the sum of squares of each matrix is actually calculated and the matrices are left intact. The Metropolis algorithm is then applied to determine whether the change (the new formulation) is accepted or not based on the change of cost function and the current effective temperature. This is different from the SIMOPT algorithm in that there is no need to carry out the student-*t* test and Fisher *F*-test for each matrix after any move in MULTIREG. If the move is accepted, then the MULTIREG will delete term B from the formulation and add in term A. The matrices are then transformed using stepwise regression methods to reflect this change. If the move is not accepted, the MULTIREG will choose another pair of terms, one from the bank of terms and the other from the current formulation, and repeat the attempted exchanges. The MULTIREG algorithm stops after satisfying the termination conditions listed in Section 2 and the form of the engineering EOS is then determined. Nonlinear regressions are then performed for each individual fluid to find the coefficients that optimize its representation of experimental data.

It is interesting to note that only a small amount of data for each fluid is sufficient to generate good results using the MULTIREG algorithm. These data should be representative for certain thermodynamic states, such as the vapor–liquid equilibrium (VLE) boundary, the gas and liquid phase densities, etc. In this work, the typical number of data selected was between 150 and 200 for each fluid, much smaller than the amount of data required to develop a reference quality EOS.

4. Simultaneously optimized engineering equation of state

A 14-term engineering equation of state has been obtained by using the simultaneous optimization algorithm MULTIREG for a total of 13 non- and weakly polar fluids, five polar fluids and four associating fluids. There were 184 polynomial and exponential terms present in the bank of possible terms and no special critical region terms were included. The resulting equation has the following form for the dimensionless Helmholtz energy:

$$\Phi = \Phi^{\mathrm{id}}(\delta, t) + \Phi^{\mathrm{r}}(\delta, t) \quad (15)$$

$$\Phi^{\mathrm{r}}(\delta, \tau) = \sum_{m=1}^{6} a_m \delta^{i_m} \tau^{j_m} + \sum_{m=7}^{14} a_m \delta^{i_m} \tau^{j_m} \exp(-\delta^{k_m}) \quad (16)$$

where a_m are the coefficients in the residual part of Helmholtz energy, and i_m, j_m and k_m are exponents of density and temperature terms which are presented in Table 1.

Coefficients for Eq. (16) for non- and weakly polar fluids such as methane, ethane, ethylene, propane, isobutane, *n*-butane, *n*-pentane, *n*-hexane, *n*-octane, cyclohexane, benzene, toluene and nitrogen are given in Table 2. Coefficients for Eq. (16) for polar and associating fluids such as carbon dioxide, R32, R125, R134a, ammonia, methanol, ethanol, 1-propnaol, and water are listed in Table 3.

Two simultaneously optimized EOS of Span and Wagner [11,14] were used to compare the accuracy of Eq. (16). Each of their equations, namely the SW-NP and SW-PL, contains 12-terms and was developed solely for non-polar and polar fluids, respectively. Table 4 summarizes the values of average absolute deviation (AAD) obtained when applying Eq. (16) and the SW-NP to selected experimental data sets for the 13 non- and weakly polar fluids. Aromatic hydrocarbons such as benzene and toluene were not included in Span and Wagner's work published to date, therefore only calculations from Eq. (16) are given. Table 5 presents the values of AAD obtained by applying Eq. (16) and the SW-PL to the nine polar and associating fluids. Only calculations from Eq. (16) for associating fluids such as alcohols and water are given since they are not included in Span and Wagner's work.

The databases of the fluids studied vary greatly [29]. For fluids such as methane, ethane, propane and nitrogen, there are extensive accurate experimental measurements which cover ranges from the gas phase to the critical regions and

Table 1
Exponents of the simultaneously optimized engineering equation of state

m	i_m	j_m	k_m
1	1	1.5	0
2	1	0.25	0
3	1	1.25	0
4	3	0.25	0
5	7	0.875	0
6	2	1.375	0
7	1	0.0	1
8	1	2.375	1
9	2	2.0	1
10	5	2.125	1
11	1	3.5	2
12	1	6.5	2
13	4	4.75	2
14	2	12.5	3

Table 2
Coefficients of the simultaneously optimized equation of state for non- and weakly polar fluids

m	a_m						
	Methane	Ethane	Ethylene	Propane	Isobutane	*n*-Butane	*n*-Pentane
1	1.25595787×10^{0}	1.32031629×10^{0}	$8.42278605 \times 10^{-1}$	$9.70439249 \times 10^{-1}$	1.18083775×10^{0}	1.18936994×10^{0}	2.20261753×10^{0}
2	$8.48007435 \times 10^{-1}$	$9.47177394 \times 10^{-1}$	$8.65139678 \times 10^{-1}$	$9.73671323 \times 10^{-1}$	$9.46903331 \times 10^{-1}$	1.05407451×10^{0}	1.07797592×10^{0}
3	$-3.00939285 \times 10^{0}$	$-3.21919278 \times 10^{0}$	$-2.79801027 \times 10^{0}$	$-2.96661981 \times 10^{0}$	$-2.90618044 \times 10^{0}$	$-3.24964532 \times 10^{0}$	$-3.82130221 \times 10^{0}$
4	$5.99544996 \times 10^{-2}$	$7.47287278 \times 10^{-2}$	$6.74520156 \times 10^{-2}$	$7.84340496 \times 10^{-2}$	$8.51346220 \times 10^{-2}$	$8.25263908 \times 10^{-2}$	$1.06627357 \times 10^{-1}$
5	$2.57003062 \times 10^{-4}$	$2.74919584 \times 10^{-4}$	$2.42445468 \times 10^{-4}$	$2.78440866 \times 10^{-4}$	$2.79868503 \times 10^{-4}$	$2.76467405 \times 10^{-4}$	$3.07513215 \times 10^{-4}$
6	$-2.85914246 \times 10^{-2}$	$-6.33952115 \times 10^{-2}$	$-2.74767618 \times 10^{-3}$	$-6.77622221 \times 10^{-2}$	$-1.68266335 \times 10^{-1}$	$-8.09869214 \times 10^{-2}$	$-2.84309667 \times 10^{-1}$
7	$-6.83210861 \times 10^{-2}$	$-5.17685674 \times 10^{-2}$	$-1.48602227 \times 10^{-2}$	$-8.56371936 \times 10^{-2}$	$-2.01202825 \times 10^{-1}$	$-9.38097492 \times 10^{-2}$	$-7.28441220 \times 10^{-2}$
8	$-3.47523515 \times 10^{-2}$	$3.65838926 \times 10^{-2}$	$1.29307481 \times 10^{-1}$	$1.77467443 \times 10^{-1}$	$-3.32570120 \times 10^{-2}$	$1.46213532 \times 10^{-1}$	$-4.60943732 \times 10^{-1}$
9	$1.04637008 \times 10^{-1}$	$2.57753669 \times 10^{-1}$	$3.74759088 \times 10^{-1}$	$3.91636018 \times 10^{-1}$	$2.42967225 \times 10^{-1}$	$4.01168502 \times 10^{-1}$	$8.39360011 \times 10^{-2}$
10	$-1.09884198 \times 10^{-2}$	$-1.34856586 \times 10^{-2}$	$-1.25336440 \times 10^{-2}$	$-8.03312946 \times 10^{-3}$	$-4.20931100 \times 10^{-3}$	$-1.28716120 \times 10^{-2}$	$-1.50650444 \times 10^{-2}$
11	$-1.25124331 \times 10^{-1}$	$-2.21551776 \times 10^{-1}$	$-2.33507187 \times 10^{-1}$	$-2.60385851 \times 10^{-1}$	$-2.24528572 \times 10^{-1}$	$-2.75191070 \times 10^{-1}$	$-2.03771872 \times 10^{-1}$
12	$-5.53450960 \times 10^{-3}$	$-6.89219870 \times 10^{-4}$	$1.38862785 \times 10^{-2}$	$-1.91104746 \times 10^{-2}$	$-1.41307663 \times 10^{-2}$	$-1.62708971 \times 10^{-2}$	$-7.90244277 \times 10^{-3}$
13	$-1.51182884 \times 10^{-2}$	$-4.47904791 \times 10^{-2}$	$-4.88033330 \times 10^{-2}$	$-6.31331470 \times 10^{-2}$	$-5.93401702 \times 10^{-2}$	$-7.04082962 \times 10^{-2}$	$-5.68993564 \times 10^{-2}$
14	$-2.04800000 \times 10^{-2}$	$-2.15665728 \times 10^{-2}$	$-2.38141707 \times 10^{-2}$	$-2.27769095 \times 10^{-2}$	$-2.27862942 \times 10^{-2}$	$-2.32871995 \times 10^{-2}$	$-2.99387974 \times 10^{-2}$
	n-Hexane	Benzene	Toluene	Nitrogen	Cyclohexane	*n*-Octane	
1	2.43433265×10^{0}	1.76284970×10^{0}	1.34060172×10^{0}	$9.57664698 \times 10^{-1}$	1.27436292×10^{0}	1.57750154×10^{0}	
2	1.18137185×10^{0}	1.02610647×10^{0}	1.01624262×10^{0}	$8.68692283 \times 10^{-1}$	1.15372124×10^{0}	1.15745614×10^{0}	
3	$-4.24411947 \times 10^{0}$	$-3.74263321 \times 10^{0}$	$-3.27810202 \times 10^{0}$	$-2.88536117 \times 10^{0}$	$-3.86726473 \times 10^{0}$	$-3.54867092 \times 10^{0}$	
4	$1.08655334 \times 10^{-1}$	$9.57682041 \times 10^{-2}$	$9.69209624 \times 10^{-2}$	$6.12953165 \times 10^{-2}$	$8.84627298 \times 10^{-2}$	$1.18030671 \times 10^{-1}$	
5	$2.87828538 \times 10^{-4}$	$2.59179321 \times 10^{-4}$	$2.61950176 \times 10^{-4}$	$2.55919463 \times 10^{-4}$	$2.76478090 \times 10^{-4}$	$3.02753897 \times 10^{-4}$	
6	$-2.51781047 \times 10^{-1}$	$-1.03082188 \times 10^{-1}$	$-1.58891991 \times 10^{-1}$	$1.69423647 \times 10^{-2}$	$7.26682313 \times 10^{-2}$	$-2.63074957 \times 10^{-1}$	
7	$2.16096570 \times 10^{-2}$	$1.07359246 \times 10^{-1}$	$6.28559812 \times 10^{-2}$	$-4.43639900 \times 10^{-2}$	$7.10849914 \times 10^{-2}$	$2.55299486 \times 10^{-2}$	
8	$-4.58052979 \times 10^{-1}$	$-1.12562310 \times 10^{-1}$	$-8.42364946 \times 10^{-2}$	$1.37987734 \times 10^{-1}$	$4.46376742 \times 10^{-1}$	$-1.26632996 \times 10^{-1}$	
9	$1.63940974 \times 10^{-1}$	$3.18737987 \times 10^{-1}$	$4.49701117 \times 10^{-1}$	$2.77148365 \times 10^{-1}$	$7.64476190 \times 10^{-1}$	$4.48343319 \times 10^{-1}$	
10	$-2.55034034 \times 10^{-2}$	$-3.07549016 \times 10^{-2}$	$-1.08658876 \times 10^{-2}$	$-1.44381707 \times 10^{-2}$	$-4.23520282 \times 10^{-2}$	$-9.46702997 \times 10^{-3}$	
11	$-2.47418231 \times 10^{-1}$	$-3.25082386 \times 10^{-1}$	$-3.83733669 \times 10^{-1}$	$-1.69955805 \times 10^{-1}$	$-3.96468623 \times 10^{-1}$	$-4.43927529 \times 10^{-1}$	
12	$-8.05544799 \times 10^{-3}$	$2.28099159 \times 10^{-2}$	$2.21127543 \times 10^{-2}$	$5.46894457 \times 10^{-3}$	$-1.41250071 \times 10^{-2}$	$-1.68224827 \times 10^{-2}$	
13	$-7.78926202 \times 10^{-2}$	$-7.07431076 \times 10^{-2}$	$-9.54658223 \times 10^{-2}$	$-2.87747274 \times 10^{-2}$	$-1.08371284 \times 10^{-1}$	$-1.15864640 \times 10^{-1}$	
14	$-2.69044742 \times 10^{-2}$	$-1.96809158 \times 10^{-2}$	$-1.77905259 \times 10^{-2}$	$-2.38630424 \times 10^{-2}$	$-2.50082884 \times 10^{-2}$	$-1.32417591 \times 10^{-2}$	

Table 3
Coefficients of the simultaneously optimized equation of state for polar and associating fluids

m	a_m								
	Carbon dioxide	R32	R125	R134a	Ammonia	Methanol	Ethanol	1-Propanol	Water
1	$-4.71122371 \times 10^{-1}$	$2.75866232 \times 10^{-1}$	$7.41057508 \times 10^{-1}$	1.08605179×10^{0}	$3.29159441 \times 10^{-1}$	-2.4578394×10^{0}	$-2.95455387 \times 10^{0}$	$-6.48466690 \times 10^{0}$	$3.46821920 \times 10^{-1}$
2	$9.13375599 \times 10^{-1}$	$9.26526641 \times 10^{-1}$	1.13555445×10^{0}	1.03772416×10^{0}	$8.48237019 \times 10^{-1}$	1.39060027×10^{0}	1.95055493×10^{0}	$6.34812260 \times 10^{-1}$	$5.03423025 \times 10^{-1}$
3	$-1.96793707 \times 10^{0}$	$-2.44296579 \times 10^{0}$	$-3.12563760 \times 10^{0}$	$-2.92069735 \times 10^{0}$	$-2.30706412 \times 10^{0}$	$8.56114069 \times 10^{-1}$	$-1.31612955 \times 10^{0}$	5.34271316×10^{0}	$-3.51059570 \times 10^{-1}$
4	$6.89687161 \times 10^{-2}$	$5.34289357 \times 10^{-2}$	$9.32031442 \times 10^{-2}$	$9.15573346 \times 10^{-2}$	$4.08625188 \times 10^{-2}$	$-4.20843418 \times 10^{-2}$	$-1.47547651 \times 10^{-2}$	$3.59156552 \times 10^{-2}$	$5.07004866 \times 10^{-2}$
5	$2.15658922 \times 10^{-4}$	$1.06739638 \times 10^{-4}$	$2.76844975 \times 10^{-4}$	$2.40541430 \times 10^{-4}$	$6.79597481 \times 10^{-5}$	$3.63682442 \times 10^{-5}$	$1.39251945 \times 10^{-4}$	$3.91173758 \times 10^{-4}$	$1.99939129 \times 10^{-4}$
6	$9.51876380 \times 10^{-2}$	$3.46487335 \times 10^{-2}$	$-5.64403707 \times 10^{-2}$	$-2.00239570 \times 10^{-1}$	$4.99412149 \times 10^{-2}$	$7.05598662 \times 10^{-1}$	$5.04178939 \times 10^{-1}$	$-4.42778070 \times 10^{-1}$	$-5.69888763 \times 10^{-1}$
7	$-4.91366518 \times 10^{-3}$	$9.07435007 \times 10^{-2}$	$9.63969526 \times 10^{-3}$	$-1.61424796 \times 10^{-2}$	$1.23624654 \times 10^{-1}$	$3.70573369 \times 10^{-1}$	$2.52310166 \times 10^{-1}$	$-1.33146361 \times 10^{0}$	$-1.96198912 \times 10^{-1}$
8	$7.32487713 \times 10^{-1}$	$-1.93104843 \times 10^{-1}$	$4.30480259 \times 10^{-1}$	$-2.15499979 \times 10^{-1}$	$-3.02129187 \times 10^{-1}$	2.46303468×10^{0}	1.97074652×10^{0}	1.71475104×10^{0}	$-2.02509554 \times 10^{0}$
9	$8.70918629 \times 10^{-1}$	$5.11370826 \times 10^{-1}$	$7.65668079 \times 10^{-1}$	$3.11819936 \times 10^{-1}$	$3.31747586 \times 10^{-1}$	1.50253790×10^{0}	$8.73146115 \times 10^{-1}$	$-1.20634979 \times 10^{-2}$	$-1.09353609 \times 10^{0}$
10	$-5.35917679 \times 10^{-3}$	$3.09453923 \times 10^{-3}$	$-1.13913859 \times 10^{-2}$	$1.12867938 \times 10^{-3}$	$-2.97121254 \times 10^{-3}$	$7.47553687 \times 10^{-2}$	$4.27767205 \times 10^{-2}$	$2.02582101 \times 10^{-1}$	$7.25785202 \times 10^{-2}$
11	$-4.03818537 \times 10^{-1}$	$-1.53328967 \times 10^{-1}$	$-4.41468178 \times 10^{-1}$	$-2.83454532 \times 10^{-1}$	$-1.30202073 \times 10^{-1}$	$-3.06417876 \times 10^{-1}$	$9.68966545 \times 10^{-2}$	$4.49595310 \times 10^{-2}$	$2.16072642 \times 10^{-1}$
12	$-2.40820897 \times 10^{-2}$	$-1.03816916 \times 10^{-1}$	$-2.00943884 \times 10^{-2}$	$-4.21157950 \times 10^{-2}$	$-7.45181207 \times 10^{-2}$	$-7.48402758 \times 10^{-1}$	$-8.39632113 \times 10^{-1}$	$-8.06185866 \times 10^{-1}$	$-1.01542630 \times 10^{-1}$
13	$-1.04239403 \times 10^{-1}$	$-3.8066998 \times 10^{-2}$	$-1.26041587 \times 10^{-1}$	$-8.08314045 \times 10^{-2}$	$-4.73506171 \times 10^{-2}$	$-1.01432849 \times 10^{-1}$	$-7.71828521 \times 10^{-2}$	$-1.97404896 \times 10^{-2}$	$7.46926106 \times 10^{-2}$
14	$-2.16335828 \times 10^{-2}$	$-1.16075825 \times 10^{-2}$	$-2.32331768 \times 10^{-2}$	$-1.59762784 \times 10^{-2}$	$-9.70095484 \times 10^{-3}$	$8.06830693 \times 10^{-2}$	$1.63430744 \times 10^{-2}$	$4.98309152 \times 10^{-2}$	$2.18830463 \times 10^{-3}$

Table 4
Comparisons of Eq. (16) and Span and Wagner's EOS (SW-NP) with selected experimental data of non- and weakly polar fluids

Substance	Average absolute deviation (AAD) (%)																	
	Vapor pressure		Saturated liquid density		Saturated vapor density		Single-phase density		Single-phase pressure		Isochoric heat capacity		Saturated heat capacity		Isobaric heat capacity		Speed of sound	
	This work	SW-NP	This work	SW-NP	This work	SW-NP	This work	SW-NP	This work	SW-NP	This work	SW-NP	This work	SW-NP	This work	SW-NP	This work	SW-NP
Methane	0.062	0.073	0.079	0.04	0.424	0.103	0.179	0.152	0.296	0.388	0.90	0.716	1.624	0.901	1.062	0.92	1.28	1.14
Ethane	0.424	0.18	0.089	0.049	0.141	0.389	0.524	0.647	0.622	0.471	1.108	0.929	1.498	1.982	3.055	2.884	1.99	2.13
Ethylene	0.058	0.065	0.06	0.042	0.16	0.6	0.709	0.691	6.962	6.985	2.327	1.779	n/a	n/a	2.161	2.083	0.8	0.32
Propane	0.361	0.667	0.214	0.125	0.526	0.554	0.456	0.545	4.831	3.669	6.154	8.36	1.279	3.864	1.185	1.008	1.74	0.63
Isobutane	0.132	0.81	0.155	0.193	0.365	1.154	0.502	0.411	3.09	9.47	n/a	n/a	0.30	1.763	4.963	4.56	0.02	0.01
n-Butane	0.098	0.608	0.111	0.103	0.071	0.69	0.487	0.41	1.728	1.424	1.656	0.898	0.372	0.644	3.781	3.697	1.5	0.49
n-Pentane	0.799	0.886	0.177	0.1	0.929	1.136	0.893	0.689	3.679	5.087	n/a	n/a	0.107	0.586	1.049	0.875	1.42	1.12
n-Hexane	0.204	0.594	0.158	0.204	0.357	0.931	1.114	0.999	3.80	6.764	n/a	n/a	1.834	2.02	0.785	0.706	1.03	1.26
Cyclohexane	0.096	0.711	0.177	2.639	2.638	3.231	0.205	0.545	1.757	3.455	1.892	0.809	2.612	2.019	2.247	6.366	0.19	0.34
n-Octane	0.176	0.578	0.196	0.116	0.259	0.87	0.18	0.25	3.41	4.617	0.953	1.003	n/a	n/a	0.341	0.254	0.44	1.25
Benzene	0.116		0.196		0.237		0.853		5.73		n/a		1.494		1.846		1.64	
Toluene	0.265		0.227		0.748		0.286		3.192		n/a		2.526		2.495		1.04	
Nitrogen	0.018	0.112	0.132	0.052	0.265	0.13	0.616	0.711	2.052	2.371	9.11	8.443	0.521	0.35	6.18	6.223	2.6	2.99

Table 5
Comparisons of Eq. (16) and Span and Wagner's EOS (SW-PL) with selected experimental data of polar and associating fluids

Substance	Average absolute deviation (AAD) (%)							
	Vapor pressure		Saturated liquid density		Saturated vapor density		Single-phase density	
	This work	SW-PL	This work	SW-PL	This work	SW-PL	This work	SW-PL
Carbon dioxide	0.037	0.065	0.039	0.067	0.191	0.133	0.19	0.146
R32	0.099	0.323	0.189	0.164	0.235	0.383	0.122	0.103
R125	0.017	0.044	0.072	0.091	0.175	0.21	0.096	0.085
R134a	0.10	0.333	0.147	0.163	0.247	0.363	0.108	0.101
Ammonia	0.353	0.143	0.432	0.498	0.552	0.69	0.452	0.451
Methanol	0.61		0.439		2.705		2.552	
Ethanol	0.87		0.581		1.925		0.443	
1-Propanol	0.685		0.287		2.521		1.085	
Water	0.257		0.119		0.879		0.573	
	Single-phase pressure		Isochoric heat capacity		Isobaric heat capacity		Speed of sound	
	This work	SW-PL	This work	SW-PL	This work	SW-PL	This work	SW-PL
Carbon dioxide	0.434	0.444	11.44	12.92	1.304	1.35	0.69	0.73
R32	1.018	2.091	0.512	0.692	n/a	n/a	1.12	0.66
R125	0.423	0.534	0.657	0.463	n/a	n/a	0.05	0.05
R134a	2.074	2.278	0.342	0.36	0.36	0.384	0.32	0.33
Ammonia	1.60	0.94	n/a	n/a	2.87	2.665	8.29	7.45
Methanol	3.513		n/a		n/a		n/a	
Ethanol	2.25		6.015		1.59		4.25	
1-Propanol	8.622		3.982		12.61		0.48	
Water	3.296		3.902		1.132		3.52	

the supercritical regions. However for *n*-pentane, *n*-hexane, *n*-octane and toluene, the experimental measurements are only available in limited regions and the quality of the data are not consistent. The data situation for the polar and associating fluids is not as good as for the non-polar fluids except for carbon dioxide and water. For alcohols like methanol, ethanol and 1-propanol, the experimental measurements are only available in limited regions and have questionable quality.

To elaborate the accuracy and universality of Eq. (16), we have chosen ethylene as an example of non- and weakly polar fluids, R32 (trifluoromethane) an example of polar fluids and ethanol an example of associating fluids, to demonstrate the success of the proposed simultaneous optimization algorithm. Detailed comparison on other fluids can be found in reference [29]. For water, Eq. (16) is compared to an international standard EOS by Wagner and Pruß [30] instead of experimental data.

For ethylene, the available experimental data cover the range from the triple point up to $T \approx 473$ K with pressures up to 100 MPa. A detailed review of the data sets was given by Jacobsen et al. [31] and a recent review can be found in Smukala et al. [32]. The deviations between selected experimental data by Nowak et al. [33] and the values calculated from Eq. (16) are shown in Fig. 2. In general the deviations given by Eq. (16) and the SW-NP EOS are less than 0.1%.

The available data sets of refrigerant R32 cover the regions from the triple point temperature up to $T \approx 420$ K with pressures up to 72 MPa. R32 was studied in the 1990s as an alternative refrigerant and therefore the data sets are small but with higher accuracy and consistency. An extensive review of the data was published by Tillner-Roth and Yokozeki in 1997 [34]. The deviations between the specific heat capacity along the saturation boundary by Luddecke and Magee [35] and the values calculated from Eq. (16) are plotted in Fig. 3. Overall the deviations are less than 1% except close to the critical point.

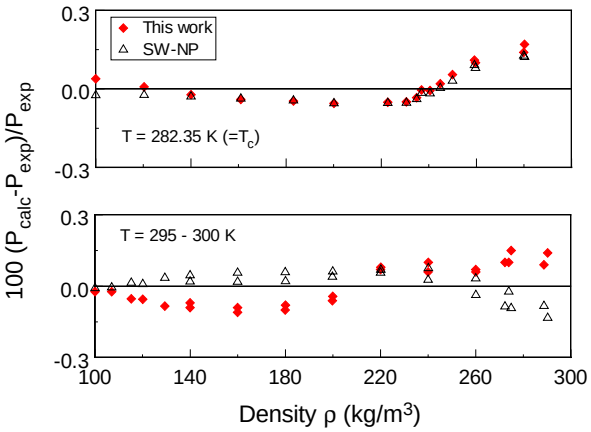

Fig. 2. Percentage deviations between the experimental $P\rho T$ data in the critical region of ethylene and values calculated in this work. Values from the Span and Wagner EOS for non-polar fluids (SW-NP) are plotted for comparison.

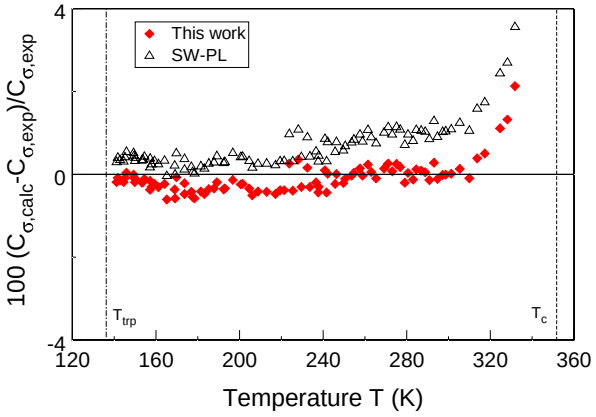

Fig. 3. Percentage deviations between the specific heat capacity along the saturation boundary data of R32 and values calculated in this work. Values from the Span and Wagner EOS for polar fluids (SW-PL) are plotted for comparison.

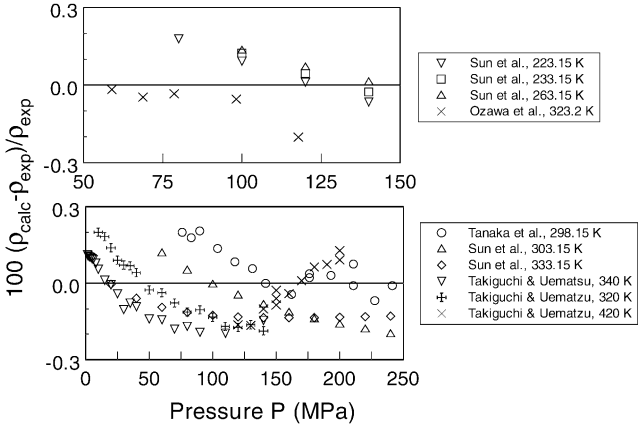

Fig. 4. Percentage deviations between the experimental $P\rho T$ data of ethanol and values calculated in this work.

For ethanol, a common solvent and renewable bio-fuel, experimental data sets are available in the region of $213 \leq T \leq 613$ K with pressures up to 250 MPa. Most of the available data sets are in the liquid state and at room temperature and pressure. Saturation liquid density data are available with good accuracy; however vapor pressure and vapor density data are not available in the low temperature region. There are no accepted values for the triple point parameters for ethanol. A detailed review of available liquid phase density data was given by Cibulka and Zikova [36]. Only recently have there been independent attempts to develop a multiparameter EOS by Dillon and Penoncello [37] and Sun and Ely [38] for ethanol. The deviations between experimental $P\rho T$ data [39–44] and values calculated from Eq. (16) are plotted in Fig. 4.

In concluding this section, Figs. 5–7 are given as examples to show the overall quality of Eq. (16) in predicting thermodynamic properties as compared to the two separate equations by Span and Wagner, i.e., the SW-NP and

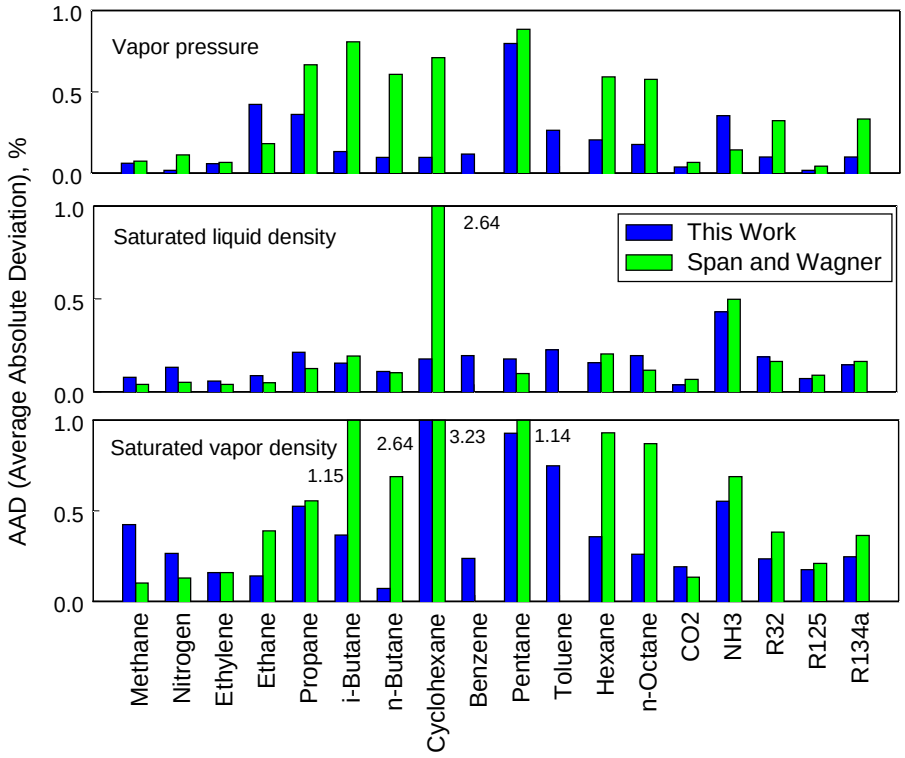

Fig. 5. Comparisons of average absolute deviations on saturation boundary calculated from Eq. (16) and the equations by Span and Wagner for considered 18 non- and weakly polar fluids and polar fluids.

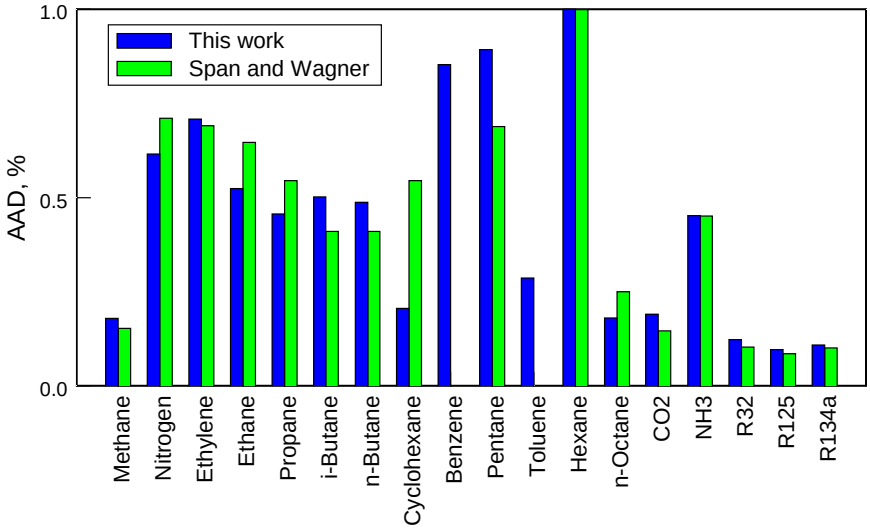

Fig. 6. Comparisons of average absolute deviations on single-phase density calculated from Eq. (16) and the equations by Span and Wagner for considered 18 non- and weakly polar fluids and polar fluids.

SW-PL. The comparisons on the vapor–liquid equilibrium boundary between the values predicted from Eq. (16) and the equations by Span and Wagner are shown in Fig. 5. The saturated liquid densities are described with similar accuracies except for cyclohexane which is predicted with larger deviations from the SW-NP equation. Eq. (16) gives a better prediction of vapor pressure and saturated vapor density for fluids with higher values of the acentric factor, however the overall deviations for 18 fluids considered in this study are similar to those obtained by Span and Wagner [11,14,15]. Comparisons of single-phase density between the values predicted from Eq. (16) and the equations by Span and Wagner are presented in Fig. 6. Eq. (16) predicts overall deviations similar to those values obtained with equations proposed by Span and Wagner for the 18 fluids. The comparisons for the isobaric heat capacity are shown in Fig. 7. As seen in Fig. 7, Eq. (16) gives much better predictions for cyclohexane, and comparable accuracies for other fluids. The equation by Span and Wagner, the SW-NP, does not give predictions for benzene and toluene.

Since the equations by Span and Wagner cannot be applied to alcohols or water, other models for associating fluids are used for comparison in this work. As an example, the comparisons of Eq. (16) with two SAFT equations for the predictions for various thermodynamic properties of ethanol are shown in Fig. 8. SAFT refers to Statistical Associating Fluids Theory originally developed by Chapman et al. [45] by applying thermodynamic perturbation theory to associating

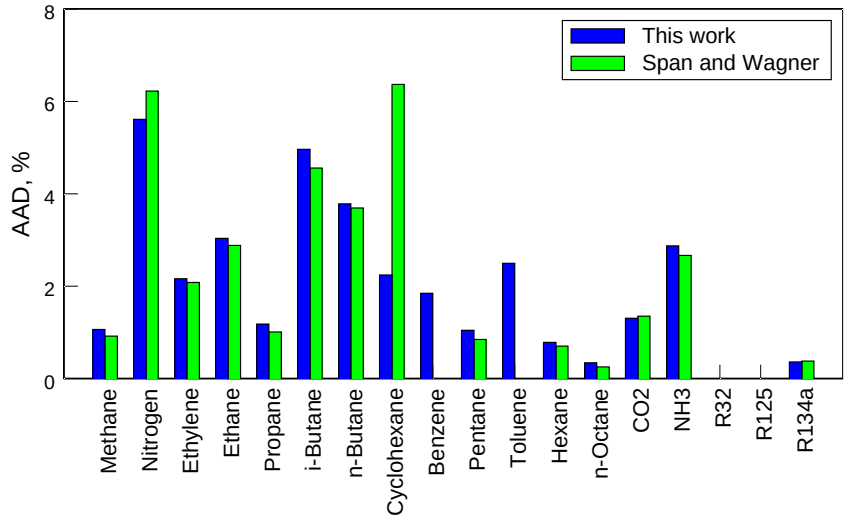

Fig. 7. Comparisons of average absolute deviations on the isobaric heat capacity calculated from Eq. (16) and the equations by Span and Wagner for considered 18 non- and weakly polar fluids and polar fluids.

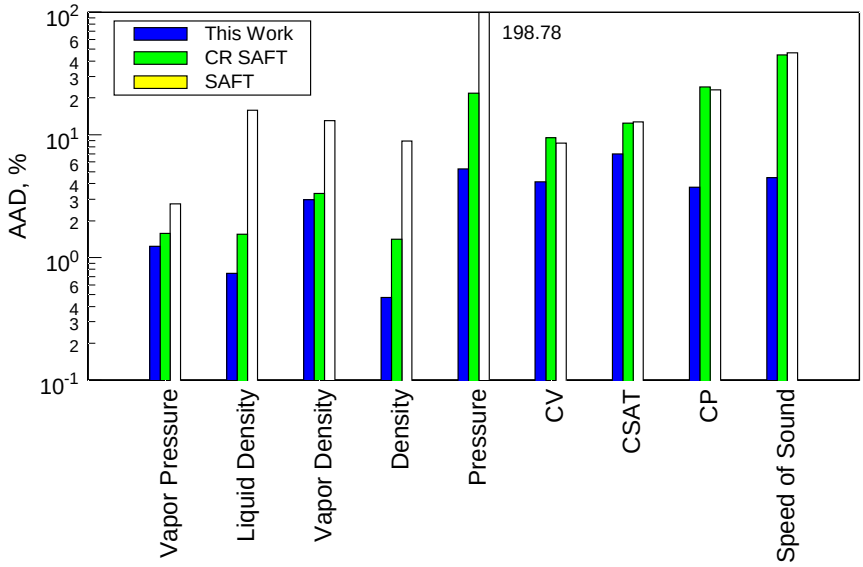

Fig. 8. Comparisons of average absolute deviations on thermodynamic properties of ethanol calculated from Eq. (16), the crossover SAFT equation by Kiselev et al., and the classical SAFT equation by Huang and Radosz.

fluids. The SAFT EOS successfully predicts the saturation boundary as well as liquid phase density for associating fluids. Huang and Radosz [46] proposed a very similar SAFT EOS which considers a polynomial expression based on molecular dynamic simulation data for the square-well potential as the dispersion force between molecule segments. Kiselev et al. [47] included the crossover formulations to the SAFT equation by Huang and Radosz (CR SAFT) in order to improve its description in the critical region.

As shown in Fig. 8, Eq. (16) shows superior accuracy for all of the thermodynamic properties of ethanol when compared to the crossover SAFT and the classical SAFT equations. The saturation boundary can be predicted with almost the same accuracy with Eq. (16) and to CR SAFT. However for single-phase density, the average absolute deviation given by Eq. (16) is three times smaller as compared to CR SAFT.

5. Conclusion

In this paper we develop a simultaneous optimization algorithm aimed at developing a universal engineering EOS with moderate accuracy. Unlike the algorithm proposed by Span and Wagner [11,13], our approach is based on simulated annealing, a stochastic algorithm. The use of simulated annealing method simplifies the optimization algorithm and requires less computing effort. Also it offers the flexibility to easily apply the algorithm to a wide range of fluids.

A structure optimized 14-term engineering EOS was obtained by applying the optimization algorithm to a total of 22 non- and weakly polar, polar fluids as well as associating fluids. Based on the overall comparisons, it can be concluded that the resulting equation, Eq. (16), yields the same accuracy as the SW-NP for the 13 non- and weakly polar fluids in the entire range of available data. We also note Eq. (16) is applicable to aromatic hydrocarbons such as benzene and toluene for which the SW-NP does not give predictions. Similarly, Eq. (16) gives the same or better accuracy as the SW-PL for the five weakly polar fluids in the entire range of available data. Eq. (16) also gives accurate predictions for associating fluids such as alcohols and water. The SW-PL cannot be applied to such fluids, as reported by Bonsen et al. in 2003 [16].

Acknowledgements

The authors are indebted to Prof. Dr. Wolfgang Wagner of Ruhr-Universität Bochum, and Prof. Dr. Roland Span of Universität Paderborn, Germany, for providing their results and lectures prior to publication. The authors would like to thank Prof. Steven Penoncello, Dr. Daniel Friend and Dr. Eric Lemmon for providing us some of the experimental data for comparisons during the course of this research. This research was supported by the U.S. Department of Energy, Office of Basic Energy Sciences, under Grant No. DE-FG03-95ER14568.

References

[1] W. Wagner, Invited Lecture: Multiparameter Equations of State in AIChE Annual Meeting, Reno, 2001.
[2] R. Span, W. Wagner, E.W. Lemmon, R.T. Jacobson, Fluid Phase Equilib. 183–184 (2001) 1.
[3] O. Redlich, J.N.S. Kwong, Chem. Rev. 44 (1949) 233.
[4] G.S. Soave, Chem. Eng. Sci. 27 (1972) 1197.
[5] D.-Y. Peng, D.B. Robinson, Ind. Eng. Chem. Fund. 15 (1976) 59.

[6] M. Benedict, G.B. Webb, L.C. Rubin, J. Chem. Phys. 8 (1940) 334.
[7] K.E. Starling, Fluid Thermodynamic Properties for Light Petroleum Systems, Houston, Gulf Publishing, 1973.
[8] E. Bender, Equations of state exactly representing the phase behavior of pure substances, in: Proceedings of the Fifth Symposium on Thermophys. Prop., ASME, New York, 1970.
[9] A. Polt, Zur Beschreibung thermodynamischer Eigenschaften reiner Fluide mit Erweiteren BWR-Gleichungen, Ph.D. Thesis, Univ. Kaiserslautern, Kaiserslautern, 1987.
[10] B. Platzer, Eine generalisierung der Zustandsgleichung von Bender Zur Berechnung von Stoffeigenschaften unpolarer und polarer Fluide und deren gemische, Ph.D. Thesis, Univ. Kaiserslautern, Kaiserslautern, 1990.
[11] R. Span, Multiparameter Equations of State—An Accurate Source of Thermodynamic Property Data, Springer-Verlag, Berlin, 2000, p. 367.
[12] U. Setzmann, W. Wagner, Int. J. Thermophys. 10 (1989) 1103.
[13] R. Span, W. Wagner, Int. J. Thermophys. 24 (2003) 1.
[14] R. Span, W. Wagner, Int. J. Thermophys. 24 (2003) 41.
[15] R. Span, W. Wagner, Int. J. Thermophys. 24 (2003) 111.
[16] C. Bonsen, R. Span, W. Wagner, AUTOFIT: a program for fully automated fitting of Helmholtz equations of state, in: Proceedings of 15th Symposium on Thermophys. Prop., Boulder, 2003.
[17] S. Kirkpatrick, J.C.D. Gelatt, M.P. Vecchi, Science 220 (1983) 671.
[18] V. Cerny, J. Opt. Theory Appl. 45 (1985) 41.
[19] N. Metropolis, A. Rosenbluth, M. Rosenbluth, A. Teller, E. Teller, J. Chem. Phys. 21 (1953) 1087.
[20] K.B. Shubert, J.F. Ely, Int. J. Thermophys. 16 (1995) 101.
[21] M.L. Huber, Comput. Chem. Eng. 18 (1994) 929.
[22] E.H.L. Aarts, P.J.M. Van Laarhoven, Philips J. Res. 40 (1985) 193.
[23] M. Lundy, A. Mees, Math. Prog. 34 (1986) 111.
[24] J. Ahrendts, H.D. Baehr, Int. Chem. Eng. 21 (1981) 557.
[25] J. Ahrendts, H.D. Baehr, Int. Chem. Eng. 21 (1981) 572.
[26] R.D. Mccarty, in: B.L. Neindre, B. Vodar (Eds.), Determination of thermodynamic properties from experimental *P–V–T* relationships, in: Experimental Thermodynamics, Experimental Thermodynamics of Non-Reacting Fluids, vol. II, Butterworth and Co. Ltd., London, 1975, Chapter 10.
[27] K.M. De Reuck, B. Armstrong, Cryogenics 19 (1979) 505.
[28] J.A. Nelder, R. Mead, Comput. J. 7 (1965) 308.
[29] L. Sun, Ph.D. Dissertation, Department of Chemical Engineering, Colorado School of Mines, Golden, 2003.
[30] W. Wagner, A. Pruß, J. Phys. Chem. Ref. Data 31 (2002) 387.
[31] R.T. Jacobsen, M. Jahangiri, R.B. Stewart, R.D. Mccarty, J.M.H. Levelt Sengers, J. White Jr., J.V. Senger, G.A. Olchowsky, K.M. De Reuck, S. Angus, R.J. Cole, B. Craven, W.A. Wakeham, International Thermodynamic Tables of the Fluid State, vol. 10: Ethylene, Blackwell, Oxford, 1988.
[32] J. Smukala, R. Span, W. Wagner, J. Phys. Chem. Ref. Data 29 (2000) 1053.
[33] P. Nowak, R. Kleinrahm, W. Wagner, J. Chem. Thermodyn. 28 (1996) 1423.
[34] R. Tillner-Roth, A. Yokozeki, J. Phys. Chem. Ref. Data 26 (1997) 1273.
[35] T.O. Luddecke, J.W. Magee, Int. J. Thermophys. 17 (1996) 823.
[36] I. Cibulka, M. Zikova, J. Chem. Eng. Data 39 (1994) 876.
[37] H.E. Dillon, S.G. Penoncello, A fundamental equation for the calculation of the thermodynamic properties of ethanol, in: Proceedings of the 15th Symposium on Thermophys. Prop., Boulder, 2003.
[38] L. Sun, J.F. Ely, Int. J. Thermophys., 2004, in review.
[39] T.F. Sun, J.A. Schouten, S.N. Biswas, Int. J. Thermophys. 12 (1991) 381.
[40] S. Ozawa, N. Ooyatsu, M. Yamabe, S. Honmo, Y. Ogino, Int. J. Thermophys. 12 (1980) 229.
[41] Y. Tanaka, T. Yamamoto, Y. Satomi, H. Kubota, T. Makita, Rev. Phys. Chem. Jpn. 47 (1977) 12.
[42] T.F. Sun, C.A. Ten Seldam, P.J. Kortbeek, N.J. Trappeniers, S.N. Biswas, Phys. Chem. Liq. 18 (1988) 107.
[43] Y. Takiguchi, M. Uematsu, Int. J. Thermophys. 16 (1995) 295.
[44] Y. Takiguchi, M. Uematsu, J. Chem. Thermodyn. 28 (1996) 7.
[45] W.G. Chapman, K.E. Gubbins, G. Jackson, M. Radosz, Ind. Eng. Chem. Res. 29 (1990) 1709.
[46] S.H. Huang, M. Radosz, Ind. Eng. Chem. Res. 29 (1990) 2284.
[47] S.B. Kiselev, J.F. Ely, H. Adidharma, M. Radosz, Fluid Phase Equilib. 183–184 (2001) 53.